

The Mutational Spectrum of the *HPRT* Gene from Human T Cells *in Vivo* Shares a Significant Concordant Set of Hot Spots with MNNG-treated Human Cells¹

Aoy Tomita-Mitchell, Losee Lucy Ling, Curtis L. Glover, Jacklene Goodluck-Griffith, and William G. Thilly²

Division of Cardiology, Children's Hospital of Philadelphia, Philadelphia, Pennsylvania 19104 [A. T.-M.]; Biological Engineering Division, Massachusetts Institute of Technology, Cambridge, Massachusetts 02139 [A. T.-M., J. G.-G., W. G. T.]; Genome Therapeutics, Corp., Waltham, Massachusetts 02453 [L. L.]; and Division of Gastroenterology, Children's Hospital of Philadelphia, Philadelphia, Pennsylvania 19104 [C. L. G.]

ABSTRACT

The preponderance of G:C to A:T transitions in inherited and somatic human mutations has led to the hypothesis that some of these mutations arise as a result of formation of *O*⁶-methylguanine in DNA. To test this hypothesis, the fine structure map of *N*-methyl-*N'*-nitro-*N*-nitrosoguanidine (MNNG)-induced mutations was determined in human lymphoblastoid cells in the human hypoxanthine-guanine-phosphoribosyltransferase (*HPRT*) gene and compared with *HPRT* mutations observed in somatic T lymphocytes from normal individuals. Human TK6 cells, which are methylguanine methyltransferase deficient (MGMT⁻), were treated with the methylating agent MNNG to create a level of *O*⁶-methylguanine in cellular DNA equal to that found in normal human tissues. A total of 676 bp of the *HPRT* gene was scanned using constant denaturing capillary electrophoresis and high-fidelity PCR. MNNG induced 14 predominant hot spots, all which were G:C to A:T transitions. Thirteen of these 14 MNNG-induced hot spots were found among the *in vivo* set, and 10 of the MNNG-induced hot spots were among 75 putative *in vivo* hot spots (mutations observed two or more times *in vivo*). Using a hypergeometric test for concordance, the MNNG-induced hot spots were found to be a significant subset of the putative *in vivo* hot spots ($P < 4 \times 10^{-7}$). The set of shared hot spots comprise some 18% of the *HPRT in vivo* hot spot spectrum and strongly suggest that MNNG-induced hot spots *in vitro* share a common mutational pathway with a significant subset of somatic mutations *in vivo*.

INTRODUCTION

Although inherited and somatic mutations are known to cause disease, the causes of these mutations are generally undefined. Mutational spectrometry, the study of quantitative patterns of mutations (1), permits the comparison of inherited and somatic mutations observed *in vivo* over identical DNA sequences to patterns of mutation induced in cells *in vitro* by suspect agents or conditions. Concordance of significant subsets of mutational hot spots is a form of evidence indicating shared mutational mechanisms.

The patterns of point mutation in the third exon of the *HPRT* gene have been observed after treatment of human lymphoblastoid cells by several mutagenic agents. These include benzo(*a*)pyrene (2), benzopyrene diol epoxides (3), chromium VI (4), UV light (5), X-rays (6), hyperbaric oxygen, hydrogen peroxide (7), the intercalating mutagen ICR-191 (8), and the SN₁ methylating agents MNNG³ and MNU (8, 9). Reports of human inherited and somatic point mutations in the *HPRT* gene (10–16) made it possible to discover how many, if any, of these are also among those induced by various mutagens in human cells. The results were

straightforward in that all mutagenic agents tested, save the two methylating agents MNNG and MNU, and UV light, induced strong mutational hot spots that were unobserved in the human *in vivo* spectrum. UV light induced two G:C to A:T transitions found in the *in vivo HPRT* spectrum but also induced multiple hot spots not found in the *in vivo* spectrum (5).

MNNG and MNU mutational spectra in *HPRT* exon 3 were, however, identical and consisted of two major G:C to A:T transition hot spots at bp 208 and 209 found in both inherited and somatic human spectra and no hot spots not reported *in vivo* (8, 9). This concordance of MNNG- and MNU-induced spectra for *HPRT* exon 3 was consistent with, but not convincing statistical evidence for, a potential mutagenic pathway sharing mechanisms of mutation with the known sequelae after chemical alkylation of DNA (17, 18).

G:C to A:T transitions overwhelmingly dominate the kinds of mutations induced by MNNG in cells of many species (8, 19–23). Although a variety of lesions are created during MNNG treatment, including N7-methylguanine, N3-methyladenine, *O*⁶-meG, and methylphosphotriesters, there is a wealth of evidence supporting *O*⁶-meG as the principle mutagenic intermediate (reviewed in Ref. 24). Alkylating agents capable of creating *O*⁶-meG are commonly found endogenously, as well as in the environment, and constitute potential causes of human mutation and cancer (25). *O*⁶-meG adducts have been detected in normal individuals at levels ranging from ~48 to 1000 adducts/cell in leukocytes (26–29). Strategies for protecting the genome from alkylation have been highly conserved in nature and include *O*⁶-meG-DNA methyltransferases (MGMT), which directly and specifically repair *O*⁶-meG adducts (30, 31), and the mismatch repair heterodimer MutSα (composed of MSH2 and MSH6; Ref. 32).

To test the hypothesis that *O*⁶-meG is an important mutagenic intermediate *in vivo*, human cells (MGMT⁻) were treated with MNNG to create *O*⁶-meG adducts at levels comparable with that observed in human tissues, and the size of the *HPRT* sequence scanned was extended to include 676 bp of coding regions and splice sites of exons 2–8 of the *HPRT* gene. This provided the opportunity to compare the MNNG-induced mutational spectrum with that observed in humans *in vivo* with greater statistical rigor. As a necessary control, the background mutational spectrum derived from untreated cells after 60 doublings was also determined.

MATERIALS AND METHODS

Cell Culture. TK6 B-lymphoblastoid cells were grown in suspension cultures using 7-liter spinner flasks in RPMI 1640 (Life Technologies, Inc., Grand Island, NY) supplemented with 5% horse serum (Life Technologies, Inc.) in a 37°C water jacket incubator with 5% CO₂. Cells were passaged by daily dilutions to 2.5–5 × 10⁵ cells/ml (33).

Untreated Cultures. Untreated cultures were started from 10³ cells of a TK6 stock culture with an *HPRT* mutant fraction of 2 × 10⁻⁶. Three cultures were then selected and expanded to 2.4 × 10⁹ cells in 7-liter tanks and maintained in exponential growth for 60 generations (48 days). Mutant fractions and plating efficiency were determined (34) by plating aliquots from each culture with and without 6TG (Sigma Chemical Co., St. Louis, MO) every 6 days. On day 48, 6TG was added to a final concentration of 1 μg/ml to select for *HPRT*⁻ mutants. These observations were used to calculate the background or “spontaneous” mutation rate (33).

Received 3/27/03; revised 6/13/03; accepted 6/27/03.

The costs of publication of this article were defrayed in part by the payment of page charges. This article must therefore be hereby marked *advertisement* in accordance with 18 U.S.C. Section 1734 solely to indicate this fact.

¹ Supported by grants from the National Institute for Environmental Health, Sciences; PO1-ES07168-05, P42-ES04675, P01-ES01640, and the Department of Energy; and DE-FG02-86ER60448.

² To whom requests for reprints should be addressed, at Biological Engineering Division, 21 Ames Street, Room 16-743, Massachusetts Institute of Technology, Cambridge, MA 02139. Phone: (617) 253-6221; Fax: (617) 258-5424; E-mail: thilly@mit.edu.

³ The abbreviations used are: MNNG, *N*-methyl-*N'*-nitro-*N*-nitrosoguanidine; CDCE, constant denaturant electrophoresis; DGGE, denaturing gradient gel electrophoresis; MNU, *N*-methylnitrosourea; *HPRT*, hypoxanthine-guanine phosphoribosyl transferase; *O*⁶-meG, *O*⁶-methylguanine.

MNNG-treated Cultures. Six cultures of TK6 cells (3.5×10^9 cells each in 7-liter tanks) were grown for a day with 100 μ l of 100% ethanol to ensure that doubling times were unaffected by the presence of ethanol. Twenty microliters of 14 μ M MNNG (Sigma Chemical Co.) were added to four cultures of cells for a final concentration of 40 nM MNNG for 1.5 h. Two cultures were kept as untreated background controls. After incubation with MNNG for 1.5 h, cells were resuspended in fresh media. An aliquot of cells was drawn from each flask at the time of resuspension to determine the cell survival for each MNNG-treated and control culture. After cultures had resumed exponential growth, *HPRT*⁻ mutants from untreated and MNNG-treated cultures were selected *en masse* by the addition of 1 μ g/ml 6TG.

Previous studies on TK6 cells treated with MNNG using the described protocol determined a relationship of $1-1.25 \times 10^4$ *O*⁶-meG adducts per mM MNNG (35). [It should be noted that the TK6 cell line does not express a detectable level of MGMT; Ref. 36.] The concentration of 40 nM MNNG created ~ 400 *O*⁶-meG adducts per cell, simulating the midrange of *O*⁶-methylguanine levels found in DNA of human organs (26-29).

Mutational Spectrometry. DNA was isolated from the mixed 6TG^R population and analyzed using high-fidelity PCR coupled with constant denaturing CDCE or DGGE (3, 37, 38). *HPRT* mutant hot spots (39) at fractions $\geq 0.4\%$ of the total mutant set were detected and measured as peaks (CDCE) or bands (DGGE) and subsequently isolated and sequenced (3, 37, 38). Primers used for the eight separate target sequences covering exons 2-8 and their splice sites have been published previously (39). These eight sequences comprise 541 of the 657 bp *HPRT* coding region. An additional 135 bp were located in intronic splice sites.

Statistical Analysis. Comparisons between groups were performed using Fisher's exact hypergeometric test (40). The *P* for concordance was calculated in a 2 \times 2 setting.

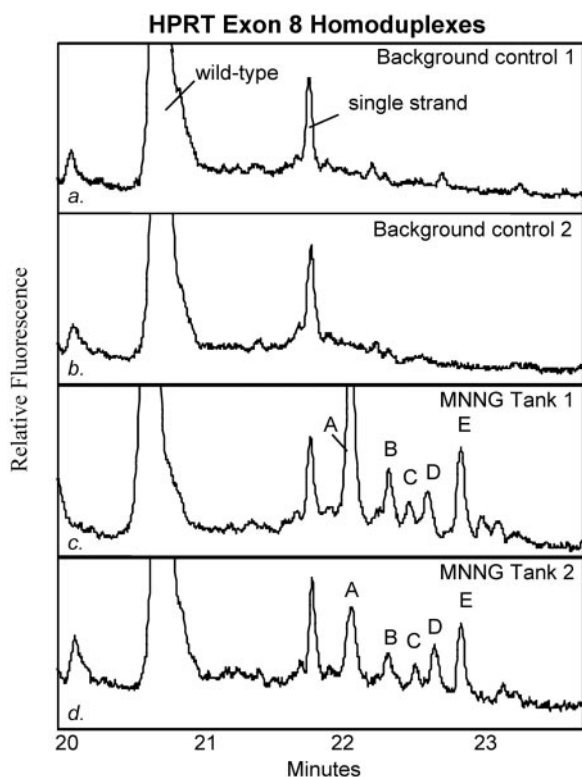


Fig. 1. a, and b, CDCE trace for exon 8 target sequence showing PCR-induced background noise in two independent experiments. c and d, CDCE trace for *HPRT* exon 8 target sequence showing MNNG-induced mutant peaks from two independent cultures [a known copy number of mutant exon 8 sequence eluting at 16 min (data not shown) was included as an internal standard to permit calculation of mutant fractions for each peak observed].

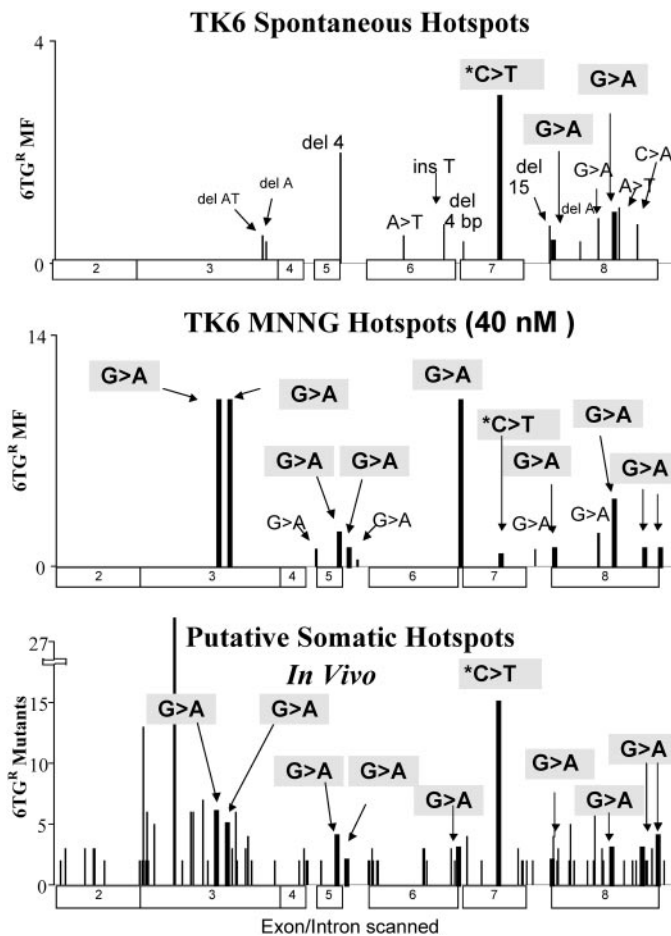


Fig. 2. Mutations in the 676 bp scanned in the *HPRT* gene (exon 2-8 and flanking introns). a, spontaneous *in vitro* mutational spectrum (% 6TG^R mutant fraction). b, MNNG-induced *in vitro* mutational spectrum (% 6TG^R mutant fraction). c, *in vivo* mutational hot spots (number of 6TG^R mutations). Hot spots shared *in vitro* and *in vivo* are represented by bold lines. Boxes on the X axis numbers indicate exons.

RESULTS

Spontaneous Cell Cultures. The doubling times for the three cultures were 17.4 ± 0.5 h (mean \pm SD). Untreated cultures reached a mutant fraction of $1.8 \pm 0.3 \times 10^{-5}$ (mean \pm SD) after 60 doublings. The background or spontaneous mutation rate, determined by least squares linear regression by plotting the mutant fraction as a function of doublings, was $2.7 \times 10^{-7} \pm 0.3 \times 10^{-7}$ (mean \pm SD) per cell doubling (33).

Cell survival for MNNG-treated cultures was $67 \pm 3\%$ (mean \pm SD), and the MNNG-induced mutant fraction was $2.4 \pm 0.2 \times 10^{-5}$ (mean \pm SD). The outcomes of both spontaneous and MNNG-treated cultures were consistent with previous experiments using bulk cultures of exponentially growing TK6 cells (7, 8, 35, 41).

Mutational Spectrometry. As an illustration of the results of mutational spectrometry, CDCE electropherograms of the PCR background trace from *HPRT*⁺ cells (negative control) and the sets of mutant peaks observed for exon 8 after treatment with MNNG are shown in Fig. 1.

Mutational Hot Spots of the Human *HPRT* Gene

Spontaneous Hot Spots *in Vitro*. Fourteen reproducible spontaneous hot spots (mutations present in the 6TG^R cell population at a level of $\geq 0.4\%$) within the 676-bp sequences scanned accounted

Table 1 Summary of spontaneous HPRT hot spots in human TK6 cells after 60 *in vitro* doublings

bp Position ^a	Exon/intron ^b	Sequence context ^c	Mutation type ^d	Point mutant fraction ^e	Phenotypic Δ ^f	Somatic mutations ^g	Germ-line mutations ^h
258-9 or 257-8	Exon 3	G AA(TA)GA AAT AG	del 2	5.E-03	Frameshift	0	0
265	Exon 3	GA AAT (A)GT GA	del 1	4.E-03	Frameshift	0	0
401 or 403	Exon 5	GTG G(AA gt)(aagt)tc	del 4	2.E-02	Splice site loss	0	0
435-437	Exon 6	AC(T) (T)(T)G CTT	ins T	5.E-03	Frameshift	0	0
475	Exon 6	GTC AAG GTC	A > T	7.E-03	Lys- > stop	0	0
IVS6 + (2-5)	Intron 6	AG g(tatg)(<u>atag</u>) aca	del 4	4.E-03	Splice site loss	0	0
508	Exon 7	CCA CGA AGT <u>TT GTT (G (GA TTT GAA ATT</u>	C > T	3.E-02	Arg- > stop	15	6
538 or 539	Exon 8	<u>CCA) G)AC AAG TTT GTT</u> GTA	del 15	7.E-03	Frameshift	0	0
538	Exon 8	GTT GGA TTT	G > A	4.E-03	Gly- > Arg	2	1
556 or 557	Exon 8	GAC (A)(A)G TTT	del 1	4.E-03	Frameshift	0	0
569	Exon 8	GTA GGA TAT	G > A	8.E-03	Gly- > Glu	1	0
580	Exon 8	CTT GAC TAT	G > A	9.E-03	Asp- > Asn	3	1
581	Exon 8	CTT GAC TAT	A > T	1.E-02	Asp- > Val	1	0
594	Exon 8	GAA TAC TTC	C > A	7.E-03	Tyr- > stop	0	0

^a Column 1, mutational hot spot position (A of ATG is nucleotide 1 for mutations occurring in coding sequences).

^b Column 2, the affected exon/intron.

^c Column 3, sequence context on the untranscribed DNA strand (uppercase letters indicate coding sequences; lowercase letters indicate intron sequences). Bold characters indicate the changed bp or sequence; underlining highlights local repeat sequences.

^d Column 4, mutation type.

^e Column 5, observed mutant fraction (mf₁).

^f Column 6, expected phenotypic change.

^g Column 7, number of times the mutation was observed out of 458 6TG^R mutants from peripheral T-lymphocytes of normal individuals.

^h Column 8, number of times the mutation was observed out of 108 Lesch-Nyhan patients.

for ~10% of all spontaneous HPRT⁻ mutants (Fig. 2, Table 1). Large deletions account for an additional 40% of spontaneous mutations in TK6 cells (42). Combining these studies, we estimate that about half of all background *in vitro* HPRT⁻ mutants are accounted. For a mutant hot spot present at 0.4%, the number of independent mutations that arose in each 6-liter culture is 173 ± 29 mutations (mean ± SD). Seven of the hot spots were small insertions or deletions. Of the 7 bp substitutions, 4 were G:C to A:T transition mutations.

MNNG-induced Hot Spots *in Vitro*. Fourteen mutational hot spots were reproducibly detected and sequenced in MNNG-treated cultures, totaling ~45% of all MNNG-induced 6TG^R mutants (Fig. 2, Table 2). For an observed mutant fraction of 0.4%, the number of independently induced mutations was 203 ± mutations (mean ± SD). All hot spot sequences from MNNG-treated cultures were G:C to A:T transitions mutations.

Four hot spots, derived from MNNG-treated cells, are concordant with spontaneous hot spots. Three hotspots, at 538, 569, and 580 bp, occur at higher mutant fractions in MNNG-treated cultures than in spontaneous cultures carried for 60 doublings. The fourth hot spot, at bp 508, is a mutation at a CpG dinucleotide, and occurs at a lower mutant fraction in MNNG-treated cultures (0.7%) than in spontaneous cultures (2%). It is possible that the 508 transition arose spontaneously (*i.e.*, via deamination and/or misincorporation) and was diluted by MNNG-induced mutants before 6TG selection. However, this mutation was not present at a level > 0.4% in the untreated background controls carried alongside the MNNG-treated cultures. Because the total MNNG-induced mutant fraction is almost seven times higher than the untreated background controls, it is assumed that all four hot spots were induced by MNNG.

Somatic Hot Spots *in Vivo*. The human HPRT mutational database contains both somatic mutations of 6TG-resistant peripheral

Table 2 Summary of MNNG-induced (40 nM) HPRT hot spots in human TK6 cells

TK6 MNNG (40 nM) induced mutational hot spots.

bp Position ^a	Exon/intron ^b	Sequence context ^c	Mutation type ^d	Point mutant fraction ^e	Phenotypic Δ ^f	Somatic mutations ^g	Germ-line mutations ^h
208	Exon 3	AAG GGG GGC	G > A	1.E-01	Gly- > Arg	6	2
209	Exon 3	AAG GGG GGC	G > A	1.E-01	Gly- > Glu	5	3
IVS4-1	Intron 4	ctag AAT	G > A	1.E-02	Splice site	0	0
400	Exon 5	GTG GAA gta	G > A	2.E-02	Glu- > Lys	4	0
IVS5 + 1	Intron 5	GAA gtaa	G > A	1.E-02	Splice site	2	1
IVS5 + 5	Intron 5	taagtc	G > A	4.E-03	Splice site	1	0
IVS6 + 1	Intron 6	A AGgtat	G > A	1.E-01	Splice site	3	1
508	Exon 7	CCA CGA AGT	C > T	7.E-03	Arg- > stop	15	6
IVS7 + 5	Intron 7	taagtga	G > A	1.E-02	Splice site	1	2
538	Exon 8	GTT GGA TTT	G > A	1.E-02	Gly- > Arg	2	1
569	Exon 8	GTA GGA TAT	G > A	2.E-02	Gly- > Glu	1	0
580	Exon 8	CTT GAC TAT	G > A	4.E-02	Asp- > Asn	3	1
599	Exon 8	TTC AGG GAT	G > A	1.E-02	Arg- > Lys	3	0
IVS8 + 1	Intron 8	AAT gtaa	G > A	1.E-02	Splice site	4	0

^a Column 1, mutational hot spot position (A of ATG is nucleotide 1 for mutations occurring in coding sequences; intron mutations are represented by the intron number and donor or acceptor site).

^b Column 2, the affected exon/intron.

^c Column 3, sequence context on the untranscribed DNA strand (uppercase letters indicate coding sequences; lowercase letters indicate intron sequences). Bold characters indicate the changed bp or sequence; underlining highlights local repeat sequences.

^d Column 4, mutation type.

^e Column 5, observed mutant fraction (mf₁).

^f Column 6, expected phenotypic change.

^g Column 7, number of times the mutation was observed out of 458 6TG^R mutants from peripheral T-lymphocytes of normal individuals.

^h Column 8, number of times the mutation was observed out of 108 Lesch-Nyhan patients.

Table 3 Table of putative somatic HPRT in vivo hotspots

bp Position ^a	Mutation type ^b	Somatic mutations in vivo ^c	Sequence context ^d	bp Position ^e	Mutation type	Somatic mutations in vivo	Sequence context
41	del 9	2	GAA CCA GGT TAT GAC	404	a > t	2	aag GAT ATA
47	g > a	3	CCA GGT TAT	418	g > c	2	ACT GGC AAA
65	t > c	3	TTA TTT TGC	419	g > a	2	ACT GGC AAA
74	c > g	3	ATA CCT AAT	463	c > t	3	AAT CCA AAG
74	c > t	3	ATA CCT AAT	464	c > t	3	AAT CCA AAG
85	gg > a	2	TAT GCT GAG	464	c > g	2	AAT CCA AAG
135	gg > c	2	tag G ACT	481	g > c	3	GTC GCA AG g
135	gg > t	2	tag G ACT	484	a > c	2	GCA AG gta
143	gg > a	13	GAA CGT CTT	IVS6 + 1	gg > a	3	A AG gtat
143	g > t	2	GAA CGT CTT	486	c > g	4	cag C TTG
145	c > t	2	CGT CTT GCT	496	a > g	2	GTG AAA AGG
146	t > gg	6	CGT CTT GCT	508	c > t	15	CCA CGA AGT
146	t > c	2	CGT CTT GCT	527	c > g	3	AAG CCA GAC
151	c > t	5	GCT CGA GAT	529	g > t	2	CCA GAC T gta
194	t > c	2	GCC CTC TGT	530	a > t	2	CCA GAC T gta
197	g > a	29	CTC TGT GTG	IVS7 + 1	g > t	2	GAC T gtaa
197	gg > t	6	CTC TGT GTG	538	gg > a	2	GTT GGA TTT
207	f -	7	AA(G GGG GG)C TAT	539	gg > a	4	GTT GGA TTT
207	f + 1	2	AA(G GGG GG)C TAT	542	t > a	2	GGA TTT GAA
208	gg > a	6	AAG GGG GGC	543	t > g	3	GGA TTT GAA
209	gg > a	5	AAG GGG GGC	551	c > t	5	ATT CCA GAC
211	gg > c	3	AAG GGG GGC	551	c > g	2	ATT CCA GAC
212	gg > a	6	GGG GGC TAT	554	a > t	2	CCA GAC AAG
213	f - 1	2	GGGCTA	563	t > a	2	TTT GTT GTA
222	c > a	3	AAA TTC TTT	568	g > c	2	GTA GGA TAT
222	c > g	4	AAA TTC TTT	568	gg > a	7	GTA GGA TAT
233	t > c	2	GAC CTG CTG	573	t > a	3	GGA TAT GCC
295	t > g	2	GAT TTT ATC	574	g > c	2	TAT GCC CTT
325	c > t	2	GAC CAG TCA	580	gg > a	3	CTT GAC TAT
368	c > g	3	CTC TCA ACT	586	a > c	2	TAT AAT GAA
IVS4 + 1	gg > a	2	AAG gtat	592	t > g	2	GAA TAC TTC
IVS4 + 2	t > a	2	AAG gtag	599	gg > a	3	TTC AGG GAT
389	t > a	2	AAT GTC TTG	601	g > t	2	AGG GAT TTG
400	gg > a	4	GTG GAA gta	602	a > t	2	AGG GAT TTG
IVS5 + 1	gg > a	2	GAA gtaa	606	g > c	3	GAT TTG AAT
IVS5 - 1	g > a	2	aaag GAT	IVS8 + 1	g > a	5	AAT gtaa
403	gg > a	2	aag GAT ATA	IVS8 + 1	g > a	5	AAT gtaa
404	a > g	3	aag GAT ATA				

^a Column 1, hot spot position (A of ATG is nucleotide 1 for mutations occurring in coding sequences; intron mutations are represented by intron number and donor or acceptor site).

^b Column 2, mutation type on the untranscribed DNA strand.

^c Column 3, number of times the hot spot mutation was observed out of 458 6TG^R mutants from peripheral T lymphocytes of normal individuals.

^d Column 4, sequence position. Bold characters indicate the changed bp or sequence.

^e Columns 5–8, Columns 1–4 repeated.

blood T-lymphocytes (10–14, 16)⁴ and inherited mutations (10, 15). 458 somatic point mutations (bp substitutions and ≤20 bp insertion/deletions) from normal, unexposed individuals and 108 inherited point mutations from Lesch-Nyhan patients have been reported in this database for the 676 bp scanned by CDCE/DGGE. [Gout patients were excluded because even 1% of normal HPRT activity can lead to toxic effects with the addition of 6TG (43), and inherited mutations related to Lesch-Nyhan syndrome may be more comparable with 6TG selected mutants than those associated with familial gout.] The somatic set contained 75 putative *in vivo* hot spots (Table 3), herein defined by two or more independent occurrences (2 of 458 somatic mutations or the equivalent of 0.4%). We estimated that the probability for any point mutation to be observed twice was 8.4% for a distribution across 676 bp × five possible point mutations (3 bp changes and two possible frameshifts +/- 1 bp). Our definition of a hot spot requires that of the 75 point mutations so designated, perhaps 6 would have been expected by chance as opposed to resulting from a higher than average mutation rate.

The Spontaneous *in Vitro* Set. When the 75 somatic *in vivo* putative hot spots were compared with the 14 spontaneous hot spots in TK6 cells, only 3, all G:C to A:T transitions, were found to be concordant. To determine whether these three mutations could have been concordant by chance, we used Fischer's exact hypergeometric test to determine the probability that any 3 of 14 spontaneous hot spots

could have overlapped with 75 somatic hot spots (40). Only mutations reported previously were used for the population number. At least 600 different HPRT⁻ point mutations that occur within the regions scanned in this study have been published previously. With 600 phenotypically observable mutations possible, the null hypothesis that 3 of 14 *in vitro* spontaneous hot spots were concordant by chance with 3 of 75 *in vivo* hot spots could not be rejected ($P > 0.15$).

Unlike the TK6 spontaneous mitochondrial point mutational spectrum, which was found previously to be highly concordant with mutational hot spots observed in human tissues *in vivo* (44), the spontaneous nuclear point mutational spectrum shares few mutational hot spots with the human *in vivo* set. Presumably different pathways drive spontaneous nuclear mutations under the cell culture conditions of this study than are found in human T cells or their precursors.

The MNNG-induced *in Vitro* Set. In contrast, 10 of 14 MNNG-induced hot spots were observed as somatic hotspots, *i.e.*, were reported as two or more independent events, and 13 of 14 were observed at least once in the somatic *in vivo* mutation database. The null hypothesis that, with 600 possible mutations, 10 of 14 MNNG-induced hot spots *in vitro* were concordant with 10 of 75 *in vivo* hot spots by chance was rejected ($P < 4 \times 10^{-7}$).

The possibility that the hot spot concordance was not determined by the mutagenic pathway but was instead attributable to the kind of mutation created was also tested. To determine whether the concordance held within the set of G:C to A:T transitions in the HPRT gene, the population number was reduced to 86 phenotypically observable

⁴ B. Glickman, personal communication.

Table 4 Table of putative *in vivo* G:C to A:T hotspots

bp Position ^a	Mutation type ^b	Somatic mutations <i>in vivo</i> ^c	Sequence context ^d	CpG or CNG site ^e	MNNG hotspot ^f
47	g > a	3	CCA GGT TAT		
74	c > t	3	ATA CCT AAT		
85	g > a	2	TAT GCT GAG		
143	g > a	13	GAA CGT CTT	CpG	
145	c > t	2	CGT CTT GCT		
151	c > t	5	GCT CGA GAT	CpG	
197	g > a	29	CTC TGT GTG	CTG	
208	g > a	6	AAG GGG GGC		MNNG
209	g > a	5	AAG GGG GGC		MNNG
212	g > a	6	GGG GGC TAT		
325	c > t	2	GAC CAG TCA	CAG	
IVS4 + 1	g > a	2	AAG gtat		
400	g > a	4	GTG GAA gta		MNNG
IVS5 + 1	g > a	2	GAA gtaa		MNNG
IVS5 - 1	g > a	2	aaag GAT		
403	g > a	2	aag GAT ATA		
419	g > a	2	ACT GGC AAA		
463	c > t	3	AAT CCA AAG		
464	c > t	3	AAT CCA AAG		
IVS6 + 1	g > a	3	A AG gtat		MNNG
508	c > t	15	CCA CGA AGT	CpG	MNNG
538	g > a	2	GTT GGA TTT		MNNG
539	g > a	4	GTT GGA TTT		
551	c > t	5	ATT CCA GAC	CAG	
568	g > a	7	GTA GGA TAT		
580	g > a	3	CTT GAC TAT		MNNG
599	g > a	3	TTC AGG GAT		MNNG
IVS8 + 1	g > a	5	AAT gtaa		MNNG
IVS8 + 5	g > a	2	gtaagta		

^a Column 1, hotspot position (A of ATG is nucleotide 1 for mutations occurring in coding sequences; intron mutations are represented by intron number and donor or acceptor site.

^b Column 2, mutation type on the untranscribed DNA strand.

^c Column 3, number of times the hotspot mutation was observed out of 458 6TG^R mutants from peripheral T-lymphocytes of normal individuals.

^d Column 4, sequence position. Bold characters indicate the changed basepair or sequence.

^e Column 5, hotspots at CpG or CNG sites.

^f Column 6, hotspots induced by MNNG *in vitro*.

G:C to A:T mutations that have been reported previously and fell within the CDCE/DGGE scanned regions. The null hypothesis that of 86 possible G:C to A:T mutations, 10 of 14 MNNG-induced hot spots were concordant with 10 of 29 *in vivo* hot spots (Table 4) by chance was still rejected ($P < 0.002$). The concordance suggested that the MNNG-induced hot spots comprised, therefore, a considerable non-random and reproducible subset of the 29 reported G:C to A:T hot spots of the *in vivo* somatic set.

Inherited Mutations *in Vivo*. Because of the small number of reported inherited mutations (currently only 108 Lesch-Nyhan patients), identification of germ-line hot spots could not be determined. However, 3 of 14 spontaneous hot spots and 9 of 14 MNNG-induced hot spots were observed at least once in the inherited set (Tables 1 and 2). It is interesting to note that the three spontaneous hot spots (bp 508, 538, and 580) observed in the germ line were also among the 4 hotspots shared by the *in vitro* sets.

DISCUSSION

Mutational hot spots have been demonstrated to be dependent on the duration and concentration of mutagen exposure (2). Thus, special effort was made to simulate human *in vivo* conditions in human cells *in vitro*, with regard to the level of *O*⁶-meG in cellular DNA. It was determined previously that treatment with 40 nM MNNG in MGMT-deficient TK6 cells would create ~400 *O*⁶-meG adducts per cell (35), within the midrange of *O*⁶-meG steady-state levels observed in normal human organs (26–29).

The Concordant Set. The 10 *in vivo* T-cell mutational hot spots concordant with the MNNG-induced spectrum support the hypothesis

that a significant subset of somatic *in vivo* hot spots share a mutational pathway with MNNG-induced mutations. These 10 G:C to A:T hotspots account for 18% (48 of 265) of all point mutations occurring as putative hot spots in T cells and 33% (48 of 145) of the set of G:C to A:T hot spots *in vivo* (see Table 4). Because there is strong evidence that MNNG acts via *O*⁶-meG, the shared mutational pathway could involve reaction with one or more SN₁ methylating agents that would be expected to create a distribution of *O*⁶-meGs in the *HPRT* gene similar to that created after exposure to MNNG.

Although no endogenous chemical has yet been demonstrated to create *O*⁶-meG in DNA (45–47), there is little doubt that it occurs at measurable levels in human tissues or DNA (26–29). The source of the *in vivo* *O*⁶-meG is unknown. Many DNA methylating agents can be formed by reaction of endogenous amines with N₂O₃ (reviewed in Ref. 48). Exogenous methylating agents include a variety of methyl-N-nitrosamines in tobacco smoke, nitrate-cured meat, and red wine (49, 50). The observations of this study do not, however, distinguish among the possibilities that methylating agents are of exogenous or endogenous origin or both. Although only normal individuals (*i.e.*, no known chemical or radiation exposure) were used in the somatic set of *in vivo* mutations, smokers were also included (~200 individuals were considered smokers). The smokers did not appear to bias the concordant hot spots either positively or negatively.

The Discordant Set

MNNG-induced Hot Spots not Found in the *in Vivo* Spectrum.

Four of 14 MNNG-induced hotspots were not observed two or more times among reported peripheral T-cell mutations. However, three of these were reported once among T-cell mutations, and of these, one was reported twice among inherited *HPRT* mutations, suggesting their absence from the somatic *in vivo* hot spot list results from the relatively small number of persons assayed. The single example of an MNNG-induced *in vitro* hot spot without a somatic or inherited mutation reported occurred at the final bp of the intron preceding exon 4. We note in passing that such splice site mutations are numerically underrepresented in the reported *HPRT in vivo* mutations because most reports involve cDNA sequencing, which would not identify specific splice site mutations. Other concordant hot spots may exist in unscanned exon sequences of the *HPRT* gene (119 bp) and sequences affecting gene expression or mRNA splice sites (>100 bp). Concordant mutations may also occur as less frequent events that were not detected by our mode of analysis.

In Vivo Hot Spots not Found in the MNNG Spectrum-CpG and CpNpG Sites.

The set of 19 *in vivo* G:C to A:T hot spots not found within the MNNG-induced set contains those at CpG or CpNpG sites, as well as others of unknown etiology (Table 4). Almost 23% (33 of 145; G:C to A:T mutations) of the *in vivo* G:C to A:T hot spots occurred at CpG dinucleotide sites, which are believed to be sites of enzymatic cytosine methylation and are thus susceptible to deamination and subsequent mutation (51, 52). Another 25% (36 of 145 somatic G:C to A:T mutations) occurred at CpNpG trinucleotide sites, which are also thought to be potential sites for enzymatic cytosine methylation.

The Remaining *in Vivo* Hot Spots not Found in the MNNG Spectrum.

Sixty *in vivo HPRT* hot spot mutations (two or more reported somatic mutations) were not concordant with the MNNG-induced spectrum nor with the set of CpG/CpNpG sequences. A small set of independent mutational pathways could account for them. If the single MNNG-like pathway could account for 10 of 75 hot spots, perhaps an additional half-dozen mutational pathways could account for the remainder. Among these could be unedited DNA polymerase misincorporation events during DNA replication, such as those created by the β DNA repair polymerase (53) during damage-induced DNA repair or metabolic DNA turnover (54).

In conclusion, it appears that MNNG treatment mimics a human T cell *in vivo* mutational pathway, accounting for 18% of somatic *HPRT* mutations. Whether DNA methylation is actually involved, as hypothesized, or whether endogenous or exogenous methylating agents are involved can not be determined from these data (55).

ACKNOWLEDGMENTS

We thank Drs. Wei-Ming Zheng, Pablo Herrero-Jimenez, and Stephan Morgenthaler for their assistance in the statistical analysis of this study. We also thank the reviewers for their careful reading of this study and helpful suggestions.

REFERENCES

- Benzer, S., and Freese, E. Induction of specific mutations with 5-bromouracil. *Proc. Natl. Acad. Sci. USA*, *44*: 112–119, 1958.
- Chen, J., and Thilly, W. G. Mutational spectra vary with exposure conditions: benzo[a]pyrene in human cells. *Mutat. Res.*, *357*: 209–217, 1996.
- Keohavong, P., and Thilly, W. G. Mutational spectrometry: a general approach for hot-spot point mutations in selectable genes. *Proc. Natl. Acad. Sci. USA*, *89*: 4623–4627, 1992.
- Chen, J., and Thilly, W. G. Mutational spectrum of chromium(VI) in human cells. *Mutat. Res.*, *323*: 21–27, 1994.
- Keohavong, P., Liu, V. F., and Thilly, W. G. Analysis of point mutations induced by ultraviolet light in human cells. *Mutat. Res.*, *249*: 147–159, 1991.
- Okinaka, R., Anzick, S., and Thilly, W. Denaturing Gradient Gel Electrophoretic Analysis of Specific Exons of the *HPRT* Gene from X-ray Induced Mutant Populations. In: *Molecular Mechanisms in Radiation Mutagenesis and Carcinogenesis*, pp. 151–162. Published by the European Commission, 1994.
- Oller, A., and Thilly, W. Mutational spectra in human B-cells. Spontaneous, oxygen, and hydrogen peroxide-induced mutations at the *hprt* gene. *J. Mol. Biol.*, *228*: 813–826, 1992.
- Cariello, N., Keohavong, P., Kat, A., and Thilly, W. Molecular analysis of complex human cell populations: mutational spectra of MNNG and ICR-191. *Mutat. Res.*, *231*: 165–176, 1990.
- Kinkaid, T. M. The methylnitrosourea-induced mutational spectra of cultured human lymphoblasts. *Toxicology*. Cambridge: MIT, 1993.
- Cariello, N. F., Craft, T. R., Vrieling, H., van Zeeland, A. A., Adams, T., and Skopek, T. R. Human *HPRT* mutant database: software for data entry and retrieval. *Environ. Mol. Mutagen.* *20*: 81–83, 1992.
- Cariello, N. F., Douglas, G. R., Gorelick, N. J., Hart, D. W., Wilson, J. D., and Soussi, T. Databases and software for the analysis of mutations in the human *p53* gene, human *hprt* gene and both the *lacI* and *lacZ* gene in transgenic rodents. *Nucleic Acids Res.*, *26*: 198–199, 1998.
- Burkhart-Schultz, K. J., and Jones, I. M. Deletion and insertion *in vivo* somatic mutations in the hypoxanthine phosphoribosyltransferase (*hprt*) gene of human T-lymphocytes (Published erratum appears in *Environ. Mol. Mutagen.* *31*: 195, 1998]. *Environ. Mol. Mutagen.* *30*: 371–384, 1997.
- Osterholm, A. M., and Hou, S. M. Splicing mutations at the *HPRT* locus in human T-lymphocytes *in vivo*. *Environ. Mol. Mutagen.* *32*: 25–32, 1998.
- Podlutzky, A., Osterholm, A., Hou, S., Hofmaier, A., and Lambert, B. Spectrum of point mutations in the coding region of the hypoxanthine-guanine phosphoribosyltransferase (*hprt*) gene in human T-lymphocytes *in vivo*. *Carcinogenesis (Lond.)*, *19*: 557–566, 1998.
- Jinnah, H. A., De Gregorio, L., Harris, J. C., Nyhan, W. L., and O'Neill, J. P. The spectrum of inherited mutations causing *HPRT* deficiency: 75 new cases and a review of 196 previously reported cases. *Mutat. Res.*, *463*: 309–326, 2000.
- Finette, B. A., Kendall, H., and Vacek, P. M. Mutational spectral analysis at the *HPRT* locus in healthy children. *Mutat. Res.*, *505*: 27–41, 2002.
- Loveless, A. Possible relevance of O⁶-alkylation of deoxyguanosine to the mutagenicity and carcinogenicity of nitrosamines and nitrosamides. *Nature (Lond.)*, *223*: 206–207, 1969.
- Saffhill, R., Margison, G. P., and O'Connor, P. J. Mechanisms of carcinogenesis induced by alkylating agents. *Biochim. Biophys. Acta*, *823*: 111–145, 1985.
- Coulondre, C., and Miller, J. H. Genetic studies of the *lac* repressor. IV. Mutagenic specificity in the *lacI* gene of *Escherichia coli*. *J. Mol. Biol.*, *117*: 577–606, 1977.
- Reed, J., and Hutchinson, F. Effect of the direction of DNA replication on mutagenesis by N-methyl-N'-nitro-N-nitrosoguanidine in adapted cells of *Escherichia coli*. *Mol. Gen. Genet.*, *208*: 446–449, 1987.
- Burns, P. A., Gordon, A. J., and Glickman, B. W. Influence of neighbouring base sequence on N-methyl-N'-nitro-N-nitrosoguanidine mutagenesis in the *lacI* gene of *Escherichia coli*. *J. Mol. Biol.*, *194*: 385–390, 1987.
- Richardson, K. K., Richardson, F. C., Crosby, R. M., Swenberg, J. A., and Skopek, T. R. DNA base changes and alkylation following *in vivo* exposure of *Escherichia coli* to N-methyl-N-nitrosourea or N-ethyl-N-nitrosourea. *Proc. Natl. Acad. Sci. USA*, *84*: 344–348, 1987.
- Kohalmi, S. E., and Kunz, B. A. Role of neighbouring bases and assessment of strand specificity in ethylmethanesulphonate and N-methyl-N'-nitro-N-nitrosoguanidine mutagenesis in the SUP4-o gene of *Saccharomyces cerevisiae*. *J. Mol. Biol.*, *204*: 561–568, 1988.
- Horsfall, M. J., Gordon, A. J., Burns, P. A., Zielenska, M., van der Vliet, G. M., and Glickman, B. W. Mutational specificity of alkylating agents and the influence of DNA repair. *Environ. Mol. Mutagen.* *15*: 107–122, 1990.
- Singer, B., and Kusmierek, J. T. Chemical mutagenesis. *Annu. Rev. Biochem.*, *51*: 655–693, 1982.
- Kang, H. I., Konishi, C., Eberle, G., Rajewsky, M. F., Kuroki, T., and Huh, N. H. Highly sensitive, specific detection of O6-methylguanine, O4-methylthymine, and O4-ethylthymine by the combination of high-performance liquid chromatography prefractionation, 32P postlabeling, and immunoprecipitation. *Cancer Res.*, *52*: 5307–5312, 1992.
- Kang, H., Konishi, C., Kuroki, T., and Huh, N. Detection of O6-methylguanine, O4-methylthymine and O4-ethylthymine in human liver and peripheral blood leukocyte DNA. *Carcinogenesis (Lond.)*, *16*: 1277–1280, 1995.
- Kyrtopoulos, S. A. O6-Alkylguanine-DNA alkyltransferase: influence on susceptibility to the genetic effects of alkylating agents. *Toxicol. Lett.*, *102–103*: 53–57, 1998.
- Georgiadis, P., Samoli, E., Kaila, S., Katsouyanni, K., and Kyrtopoulos, S. A. Ubiquitous presence of O6-methylguanine in human peripheral and cord blood DNA. *Cancer Epidemiol. Biomark. Prev.*, *9*: 299–305, 2000.
- Demple, B., Sedgwick, B., Robins, P., Totty, N., Waterfield, M. D., and Lindahl, T. Active site and complete sequence of the suicidal methyltransferase that counters alkylation mutagenesis. *Proc. Natl. Acad. Sci. USA*, *82*: 2688–2692, 1985.
- Pegg, A. E. Mammalian O6-alkylguanine-DNA alkyltransferase: regulation and importance in response to alkylating carcinogenic and therapeutic agents. *Cancer Res.*, *50*: 6119–6129, 1990.
- Duckett, D. R., Drummond, J. T., Murchie, A. I., Reardon, J. T., Sancar, A., Lilley, D. M., and Modrich, P. Human MutSalpha recognizes damaged DNA base pairs containing O6-methylguanine, O4-methylthymine, or the cisplatin-d(GpG) adduct. *Proc. Natl. Acad. Sci. USA*, *93*: 6443–6447, 1996.
- Oller, A. R., Rastogi, P., Morgenthaler, S., and Thilly, W. G. A statistical model to estimate variance in long term-low dose mutation assays: testing of the model in a human lymphoblastoid mutation assay. *Mutat. Res.*, *216*: 149–161, 1989.
- Furth, E., Thilly, W., Penman, B., Liber, H. I., and Rand, W. Quantitative assay for mutation in diploid human lymphoblasts using microtiter plates. *Anal. Biochem.*, *110*: 1–8, 1981.
- Goldmacher, V., Cuzick, R. J., and Thilly, W. Isolation and partial characterization of human cell mutants differing in sensitivity to killing and mutation by methylnitrosourea and N-methyl-N-nitro-N-nitrosoguanidine. *J. Biol. Chem.*, *261*: 12462–12471, 1986.
- Sklar, R., and Strauss, B. Removal of O6-methylguanine from DNA of normal and xeroderma pigmentosum-derived lymphoblastoid lines. *Nature (Lond.)*, *289*: 417–420, 1981.
- Khrapko, K., Hannekamp, J., Thilly, W., Belenkii, A., Foret, F., and Karger, B. Constant denaturant capillary electrophoresis (CDCFE): a high resolution approach to mutational analysis. *Nucleic Acids Res.*, *22*: 364–369, 1994.
- Khrapko, K., Coller, H., Andre, P., Li, X., Foret, F., Belenky, A., Karger, B., and Thilly, W. Mutational spectrometry without phenotypic selection: human mitochondrial DNA. *Nucleic Acids Res.*, *25*: 685–693, 1997.
- Tomita-Mitchell, A., Kat, A., Marcelino, L., Li-Sucholeiki, X.-C., Goodluck-Griffith, J., and Thilly, W. Mismatch repair deficient human cells: spontaneous and MNNG-induced mutational spectra in the *HPRT* gene. *Mutat. Res.*, *450*: 125–138, 2000.
- Piegorsch, W. W., and Bailer, A. J. Statistical approaches for analyzing mutational spectra: some recommendations for categorical data. *Genetics*, *136*: 403–416, 1994.
- Penman, B. W., Crespi, C. L., Komives, E. A., Liber, H. I., and Thilly, W. G. Mutation of human lymphoblasts exposed to low concentrations of chemical mutagens for long periods of time. *Mutat. Res.*, *108*: 417–436, 1983.
- Gennett, I. N., and Thilly, W. G. Mapping large spontaneous deletion endpoints in the human *HPRT* gene. *Mutat. Res.*, *201*: 149–160, 1988.
- Thilly, W. G., DeLuca, J., Hoppe, H. I., and Penman, B. Phenotypic lag and mutation to 6-thioguanine resistance in diploid human cells. *Mutat. Res.*, *50*: 137–143, 1978.
- Khrapko, K., Coller, H. A., Andre, P. C., Li, X. C., Hannekamp, J. S., and Thilly, W. G. Mitochondrial mutational spectra in human cells and tissues. *Proc. Natl. Acad. Sci. USA*, *94*: 13798–13803, 1997.
- Rydberg, B., and Lindahl, T. Nonenzymatic methylation of DNA by the intracellular methyl group donor S-adenosyl-L-methionine is a potentially mutagenic reaction. *EMBO J.*, *1*: 211–216, 1982.
- Barrows, L. R., and Magee, P. N. Nonenzymatic methylation of DNA by S-adenosylmethionine *in vitro*. *Carcinogenesis (Lond.)*, *3*: 349–351, 1982.
- Barrows, L. R., Shank, R. C., and Magee, P. N. S-adenosylmethionine metabolism and DNA methylation in hydrazine-treated rats. *Carcinogenesis (Lond.)*, *4*: 953–957, 1983.
- Tannenbaum, S., Tamir, S., de Rojas-Walker, T., and Wishnok, J. DNA damage and cytotoxicity caused by nitric oxide. Nitrosamines and related N-nitroso compounds, ACS symposium series, Washington DC, 1994.
- Bartsch, H., and Montesano, R. Relevance of nitrosamines to human cancer. *Carcinogenesis (Lond.)*, *5*: 1381–1393, 1984.
- Hecht, S. S., Carmella, S. G., Foiles, P. G., Murphy, S. E., and Peterson, L. A. Tobacco-specific nitrosamine adducts: studies in laboratory animals and humans. *Environ. Health Perspect.*, *99*: 57–63, 1993.
- Cooper, D. N., and Youssoufian, H. The CpG dinucleotide and human genetic disease. *Hum. Genet.*, *78*: 151–155, 1988.
- O'Neill, J. P., and Finette, B. A. Transition mutations at CpG dinucleotides are the most frequent *in vivo* spontaneous single-based substitution mutation in the human *HPRT* gene. *Environ. Mol. Mutagen.* *32*: 188–191, 1998.
- Muniappan, B. P., and Thilly, W. G. Polymerase β creates APC mutations found in human tumors. *Cancer Res.*, *62*: 3271–3275, 2002.
- Pele, S. R. Metabolic DNA in ciliated protozoa, salivary gland chromosomes, and mammalian cells. *Int. Rev. Cytol.*, *32*: 327–355, 1972.
- Thilly, W. G. Have environmental mutagens caused oncomutations in people? *Nat. Genet.* *34*: 255–259, 2003.

Cancer Research

The Journal of Cancer Research (1916–1930) | The American Journal of Cancer (1931–1940)

The Mutational Spectrum of the *HPRT* Gene from Human T Cells *in Vivo* Shares a Significant Concordant Set of Hot Spots with MNNG-treated Human Cells

Aoy Tomita-Mitchell, Losee Lucy Ling, Curtis L. Glover, et al.

Cancer Res 2003;63:5793-5798.

Updated version Access the most recent version of this article at:
<http://cancerres.aacrjournals.org/content/63/18/5793>

Cited articles This article cites 51 articles, 12 of which you can access for free at:
<http://cancerres.aacrjournals.org/content/63/18/5793.full#ref-list-1>

Citing articles This article has been cited by 1 HighWire-hosted articles. Access the articles at:
<http://cancerres.aacrjournals.org/content/63/18/5793.full#related-urls>

E-mail alerts [Sign up to receive free email-alerts](#) related to this article or journal.

Reprints and Subscriptions To order reprints of this article or to subscribe to the journal, contact the AACR Publications Department at pubs@aacr.org.

Permissions To request permission to re-use all or part of this article, use this link
<http://cancerres.aacrjournals.org/content/63/18/5793>.
Click on "Request Permissions" which will take you to the Copyright Clearance Center's (CCC) Rightslink site.